Chemical Engineering Journal 166 (2011) 413–419

Contents lists available at ScienceDirect

Chemical Engineering Journal

journal homepage: www.elsevier.com/locate/cej

Titania and titania nanocomposites on cellulosic fibers: Synthesis, characterization and comparative study of photocatalytic activity

Hadi Fallah Moafi, Abdollah Fallah Shojaie*, Mohammad Ali Zanjanchi

Department of Chemistry, Faculty of Science, University of Guilan, P.O. Box 1914, Rasht, Iran

ARTICLE INFO

Article history:
Received 3 August 2010
Received in revised form 13 October 2010
Accepted 27 October 2010

Keywords:
TiO_2
Nanocomposite
Co-doped
Self-cleaning
Sol–gel
Cellulosic fibers

ABSTRACT

Titania and titania nanocomposites (doped by Ag, Zr, and Ag–Zr) were coated on cellulosic fibers *via* sol–gel dip-coating method. The resulted coated-fibers were characterized by X-ray diffraction, scanning electron microscopy (SEM), energy dispersive spectroscopy (EDS), transmission electron microscopy (TEM), diffuse reflectance spectroscopy (DRS), and BET surface area measurement. Photocatalytic activity of the nanocomposites coated-fibers was determined by photomineralisation of methylene blue (MB) and eosin yellowish (EY) under UV–Vis light. The progress of photodegradation of dyes was monitored by diffuse reflectance spectroscopy. The XRD of all samples display anatase-type structure. All samples demonstrated photo-assisted self-cleaning properties when exposed of titania composites to UV–Vis irradiation. The Ag–Zr co-doped titania nanocomposite was found to be the most significant photoactive coatings in comparison with other samples. Our results showed that the synergistic action between the silver and the zirconium species in the Ag–Zr TiO_2 nanocomposite is due to both the structural and the electronic properties of the photoactive anatase phase. This report unequivocally indicates that modification of titania by co-doping is an effective method for increasing the photocatalytic activity.

1. Introduction

Titanium dioxide has the ability to degrade organic materials on its surface *via* photocatalysis in the presence of UV-light and an oxygen source (e.g., O_2/H_2O). All such photocatalysis reactions involve an initial photoexcitation process on the TiO_2 catalyst. Activation of TiO_2 semiconductors requires photons with energy greater than its band-gap energy (E_g) which falls within the UV-light range of the electromagnetic spectrum. However, though it is a good catalyst, its wide band gap (3.2 eV) limits TiO_2 use under visible light as the light source [1]. Hence, modifying it so that to be active under visible light is important for the practical application of this technique. Numerous studies have been performed to extend the absorption range of TiO_2 into the visible range. These studies include doping by metal and non-metal ions [2–6], dye photo-sensitization on the TiO_2 surface [7,8], sensitizing TiO_2 by narrow band gap semiconductor [9–11] and deposition of noble metals [1,12–15]. In particular, noble metal-modified semiconductor nanoparticles became of current importance for maximizing the efficiency of photocatalytic reactions. Noble metals doped or deposited on TiO_2 are expected to show various effects on the photocatalytic activity of TiO_2 by different mechanisms. These noble metals act separately or simultaneously depending on the photoreaction conditions. They may (i) enhance the electron–hole separation by acting as electron traps, (ii) extend the light absorption into the visible range and enhance surface electron excitation by Plasmon resonances excited by visible light and (iii) modify the surface properties of photocatalysts [1].

Currently, some investigators devoted themselves to improve the photoactivity of TiO_2 through co-doping process [16–24]. Some of these studies demonstrated that the observed high photocatalytic activity of the samples could be ascribed to a synergetic effect between doping ions. These reports indicated that modification of titania by co-doping may be an effective method for increasing the photocatalytic activity.

One of the most important applications of photocatalytic degradation processes is the development of self-cleaning materials. Several recent studies reported the promising potentials of nontoxic and inexpensive TiO_2 nanoparticles for exposing self-cleaning properties to different textile materials [25–30]. These self-cleaning materials provide promising applications in automobile windshields, windows of high-rise buildings, and other fields utilized for sterilization, deodorization, antifog, and room air cleaning. In the view point of practical application, it is very important to immobilize the fine TiO_2 particles onto suitable substrates in order to make self-cleaning application. The fabrication method accompanied with high temperature such as chemical vapor deposition (CVD), anodization and thermal oxidation of Ti metal, ultrasonic nebulization and pyrolysis, would brings about the cracking and/or peeling of the TiO_2 film because of the shrinkage during the crys-

* Corresponding author. Fax: +98 0131 3233262.
E-mail address: a.f.shojaie@guilan.ac.ir (A.F. Shojaie).

1385-8947/$ – see front matter © 2010 Elsevier B.V. All rights reserved.
doi:10.1016/j.cej.2010.10.074

tallization of deposited amorphous films. Furthermore, the heating process precludes the production of TiO_2 film on substrates with low thermal stability such as polymers [31]. In order to overcome these drawbacks involved in the high temperature process, low-temperature route to nanocrystalline TiO_2 particles or thin films based on sol–gel process have been reported [29,32].

In this work, we report the route that we developed as a facile and effective method to create self-cleaning coatings based on titania nanocomposites on cellulosic fibers. The silver, zirconium and silver–zirconium doped titania were prepared using the sol–gel method at ambient temperature. The photocatalytic performances of the coated-fibers with these materials are investigated following their characterization. To the best of our knowledge, Ag–Zr co-doped TiO_2 films for self-cleaning applications have not been reported so far.

2. Experimental

2.1. Reagents and materials

Titanium tetraisopropoxide (TIP), acetic acid, zirconium (IV) acetylacetonate, silver nitrate, methylene blue and eosin yellowish were purchased from Merck and were of analytical reagent grade and used without further purification. Deionized water was used in all experimental preparations. The used cellulosic fibers were 100% woven cotton fabric, plain construction, with a density of 144 g m^{-2} and the number of yarns 21/10 mm. The cellulosic fibers were scoured with detergent to remove wax, grease, and other chemical residues from fabrics before coating. For this purpose the cellulosic fibers were washed first by water and detergent at 80 °C for 30 min to remove the impurities and then washed several times by a large amount of deionized water. They were further cleaned in acetone (Merck) for 60 min and dried at room temperature for 24 h.

2.2. Synthesis procedure

The sol–gel method was used for the preparation of doped and co-doped TiO_2 nanocrystals. Titanium isopropoxide (TIP) was used as the precursor for titania sol preparation. In a typical synthesis, 10 ml of TIP was added to acetic acid (20 ml) with stirring. Deionized water (60 ml) was added to the mixture dropwise with vigorous stirring. TIP, acetic acid and water are in 1:10:100 molar ratios. The solution was stirred for 2 h to get a clear transparent sol. To prepare the doped and the co-doped titania sols, the above procedure was repeated. For synthesis of Ag–TiO_2, a certain amount of silver nitrate (2 mol% with respect to TIP) was dissolved in deionized water (60 ml), stirred and then was added into the mixture of TIP and acetic acid dropwise with vigorous stirring. For preparation of Zr–TiO_2, the required amount of zirconium (IV) acetylacetonate (2 mol% with respect to TIP) was treated the same way as described for Ag–TiO_2. These solutions were stirred for 2 h to get a clear transparent doped titania sol. In the synthesis procedure of Ag–Zr co-doped titania sol, 2 mol% of silver nitrate with respect to TIP and 2 mol% of zirconium (IV) acetylacetonate with respect to TIP were dissolved into deionized water under vigorous stirring and then the solution was added into the mixture of TIP and acetic acid dropwise while stirring rapidly at room temperature. The obtained co-doped sol was then stirred for 2 h to get a clear transparent sol and ready for dip-coating procedure.

2.3. Coating processes

The dip-pad-dry-cure process was employed to apply the as-prepared sols onto the fibers for the preparation of a durable layer. The cleaned substrates were dipped in the as-prepared sols for 5 min and then padded with a padder. The padded substrates were air-dried for 30 min at 100 °C and finally cured at 150 °C for 15 min in a preheated curing oven to ensure particles adhesion to the substrate surface. Finally, the impregnated fibers were rinsed in deionized water. During this step, the unattached particles were removed from the fiber surface.

2.4. Photocatalytic test

The photocatalytic activity of our coated-fibers was examined by exposing the samples containing pre-adsorbed methylene blue (MB) and Eosin Y to UV–Vis light.

For this purpose, 100 ml aqueous solutions (1.0×10^{-5} mol L^{-1}) of MB and Eosin Y were prepared. Both bare and coated fibers are treated in MB and Eosin Y solutions. The same amount of each sample was immersed under mild stirring in the same volume of the solution and remained overnight to complete the adsorption. The fibers were drawn out of the dyes solution and dried at room temperature. The so-obtained samples (coated-fibers) were cut into 2 cm × 2 cm pieces so that they could be fixed in the front of the integrating sphere hole of the diffuse reflectance attachment. These selected samples were exposed to UV–Vis light to test their photoactivity. The similar settings were performed in several intervals times during the test. For photocatalytic reactions, the irradiation was carried out on dry samples, by means of a high-pressure mercury lamp (HPMV 400 W, Germany). The lamp yields a spectrum ranging from ultraviolet to visible light (200–800 nm). Details of the experimental procedure were described in our previous work [26].

The photocatalytic decomposition was determined from the following equation.

$$\text{Photocatalytic decomposition} = \frac{C_0 - C}{C_0} = \frac{A_0 - A}{A_0}$$

where C_0 represents the initial concentration of the dyes on fiber surface, C the final concentration after illumination by light, A_0 the initial absorbance, and A the variable absorbance.

2.5. Characterization techniques

To investigate the morphology of the pure and coated cellulosic fibers, scanning electron microscopy (SEM) images were obtained on a Philips, XL30 equipped with an energy dispersive (EDS) microanalysis system for compositional analysis of the TiO_2-coated fibers. For the SEM and EDS analysis, samples were covered with Au. The particles sizes were obtained by transmission electron microscope (TEM) images on a Philips CM10 instrument with an accelerating voltage of 100 kV. For photodecomposition reaction, the UV–Vis reflectance spectra were recorded at room temperature by a UV-2100 Shimadzu spectrophotometer in the reflectance mode by investigating the evolution of the absorbance. The BET specific surface area of the synthesized nano-particles was determined by nitrogen adsorption at liquid nitrogen temperature on a Sibata SA-1100 surface area analyzer. X-ray diffraction measurements were recorded by a D8 Bruker Advanced diffractometer with Cu-Kα radiation, scan rate 0.02 2θ/s and within a range of 2θ of 10–70° at room temperature.

3. Results and discussion

3.1. Morphological and compositional analysis

Surface morphology of the bare fibers and the fibers after coating with TiO_2 and doped TiO_2 were studied by SEM (Fig. 1). Fig. 1a shows the surface of the pristine fibers. Fig. 1b shows the treated fibers with TiO_2 after being washed with deionized water. They

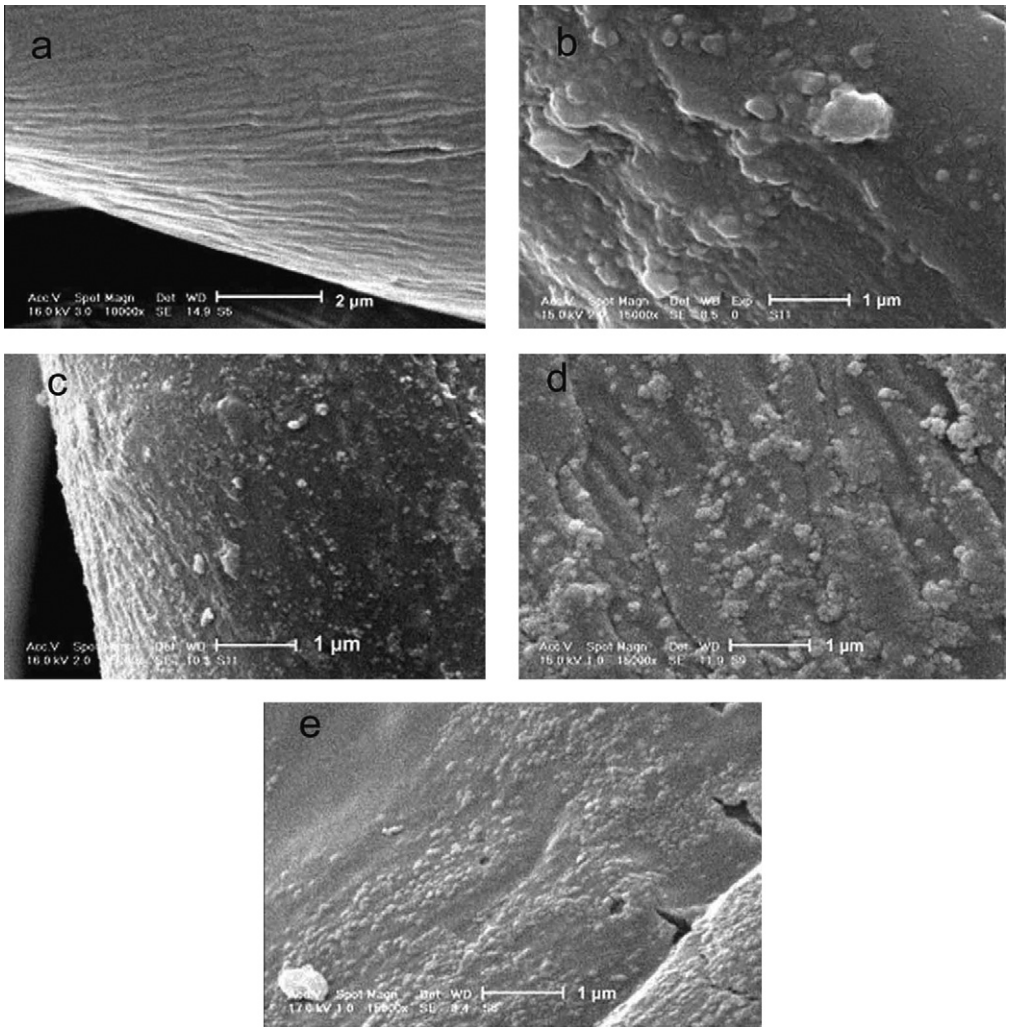

Fig. 1. SEM images of: (a) pure cellulosic fiber, (b) TiO_2-coated fiber, (c) Ag–TiO_2-coated fiber, (d) Zr–TiO_2-coated fiber and (e) Ag–Zr–TiO_2-coated fiber.

are covered by dispersed TiO_2 agglomerates. The most of them are irregularly shaped and relatively spherical with dimensions that are less than 100 nm. They are unevenly distributed over the fiber surface. Fig. 1c shows the treated fibers with Ag–TiO_2 nanosols after washing. The Ag–TiO_2 coated-fibers show a surface morphology similar to that of the bare TiO_2 coating. It can be seen that the deposited nanoparticles were composed of agglomerates of Ag–TiO_2 nanoparticles. The SEM images of the treated samples with Zr-doped and Ag–Zr co-doped TiO_2 are shown in Fig. 1d and e. These figures indicate that shape of the particles are similar to each other and likely become agglomerates of irregularly nanoparticles in general.

The elemental analysis of the treated samples was performed by EDS analysis. According to the analysis, the amount of Ti and other elements slightly varies, meaning that doping ions are occupied in the crystal structure. On the basis of this result, it is noteworthy to mention that after washing process, remarkable amount of TiO_2 and doping ions are still present on the fibers surface. This means that TiO_2 and TiO_2 nano-composites have sufficient adhesion towards the fibers in order to resist a washing process.

Fig. 2 depicts transmission electron micrographs of all samples. TEM image of TiO_2 on the coated fiber (Fig. 2a) shows that the deposited titania consists of nanoclusters with average size of ~5 nm which is consistent with the XRD results. It is noticeable that the TiO_2 nanoclusters are unevenly distributed on the fiber surface. The TEM image of Ag–TiO_2 on the surface of the fiber shows that the size of Ag–TiO_2 particles is smaller than TiO_2, mostly less than 5 nm, as seen in Fig. 2b. For Ag–TiO_2 sample, Ag species are well dispersed on the TiO_2 nanoparticles and their size distribution indicates that the vast majority is in the 5–10 nm range. However only a minor fraction of particles have larger dimensions. The small size of silver and TiO_2 nanoparticles suggests that the exposed surface area of Ag–TiO_2 coating is very large. Fig. 2c shows that Zr-doped TiO_2 sample consist of the agglomerates of primary particles with an irregular shape and size less than 5 nm which is in good agreement with XRD data. The shape of the Ag–Zr co-doped TiO_2 nanoparticles was observed as aggregated nanoparticles with average particle size of 5–8 nm (Fig. 2d). Indeed, it is demonstrated that Zr and Ag doping could inhibit the increase of TiO_2 particle size. Therefore, this result may be attributed to the presence of doping component in the TiO_2 framework. It has been demonstrated that different morphologies of TiO_2 nanocrystals have an effect on the degradation efficiency of the photocatalyst [33].

3.2. UV–Vis diffuse reflectance spectra

UV–Vis diffuse reflectance spectroscopy directly provides some insight into the interactions of the photocatalyst materials with photon energies. The reflectance spectra of TiO_2, Ag-doped TiO_2, Zr-doped TiO_2, and Ag–Zr-co-doped TiO_2 are illustrated in Fig. 3. For the sake of comparison spectrum of Degussa–TiO_2 was also included in Fig. 3. The spectrum of TiO_2 (Fig. 3d) consists of a sin-

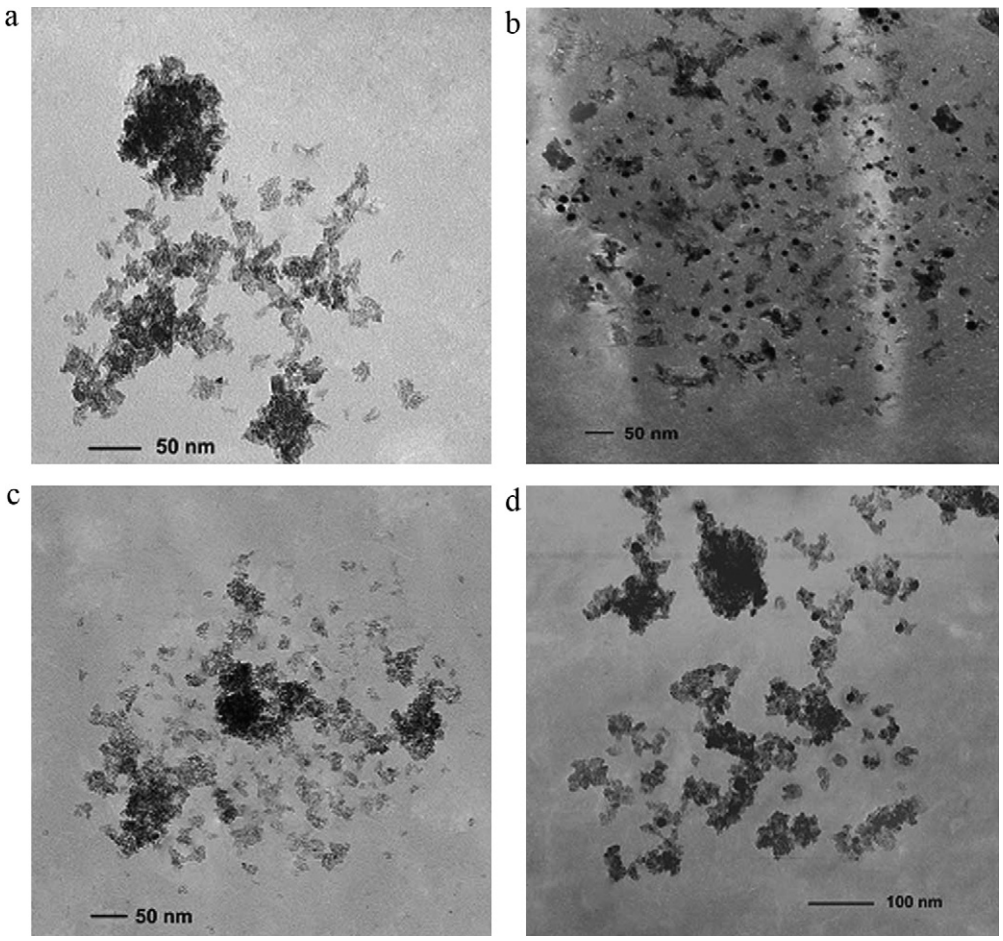

Fig. 2. TEM images of: (a) TiO_2 on cellulosic fiber, (b) Ag–TiO_2 nanocomposite on cellulosic fiber, (c) Zr–TiO_2 nanocomposite on cellulosic fiber and (d) Ag–Zr–TiO_2 nanocomposite on cellulosic fiber.

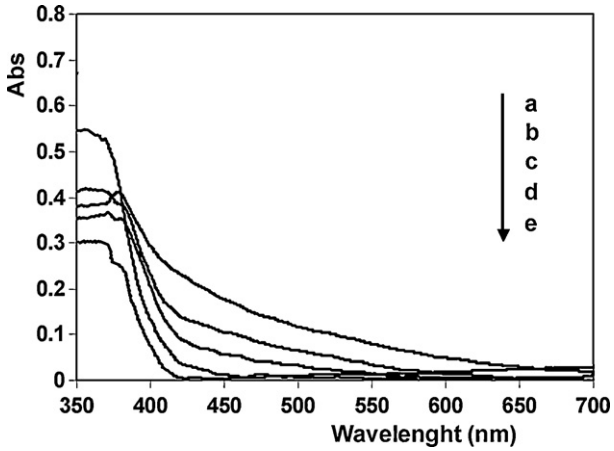

Fig. 3. Diffuse reflectance spectra of synthesized nanoparticles on cellulosic substrate: (a) Ag–Zr–TiO_2, (b) Ag–TiO_2, (c) Zr–TiO_2, (d) TiO_2 and (e) Degussa–TiO_2.

gle absorption usually ascribed to charge-transfer from the valence band (mainly formed by 2p orbitals of the oxide anions) to the conduction band (mainly formed by $3dt_2g$ orbitals of the Ti^{4+} cations) [34]. We observed a noticeable shift of the optical absorption edge for the doped TiO_2 systems towards the visible regions. Surely, this shift towards the longer wavelengths originates from the band gap narrowing of titanium dioxide by dopant ions. In the Ag–TiO_2 sample (Fig. 3b), addition of silver ions causes significant changes to the absorption spectrum of TiO_2 (Fig. 3e) resulting in absorbance from 400 nm to entire visible region. The Zr-doped TiO_2 crystals exhibited absorptions that extended to longer wavelengths (Fig. 3c). Presumably, these red shifts and reduced band gaps resulted either from defects caused by trace amounts of Zr^{4+} in the TiO_2 lattice. The red shift and reduced band gap in Ag–Zr co-doped is higher than that of other samples (Fig. 3c). The band gap energy of the doped samples was determined from the equation, $E_g = 1239.8/\lambda$, where λ is the wavelength (nm) of the exciting light (Table 1).

The difference in absorption edge wavelength for the nanocomposites coatings clearly indicates difference in the band gap of the

Table 1
Characteristics of TiO_2, Ag–TiO_2, Zr–TiO_2, and Ag–Zr–TiO_2 coatings.

Samples	Crystalline structure	Band gap energy (eV)	BET surface area (m^2/g)	Pore volume (cm^3/g)	XRD crystal size (nm)	TEM crystal size (nm)
Degussa	Anatase, Rutile	3.2	51	0.018	25	25–30
TiO_2	Anatase	3.1	350.40	0.125	8	5
Ag–TiO_2	Anatase	2.61	372.50	0.132	6	<5
Zr–TiO_2	Anatase	2.7	290.25	0.103	5	<5
Ag–Zr–TiO_2	Anatase	2.43	318.36	0.113	8	5–8

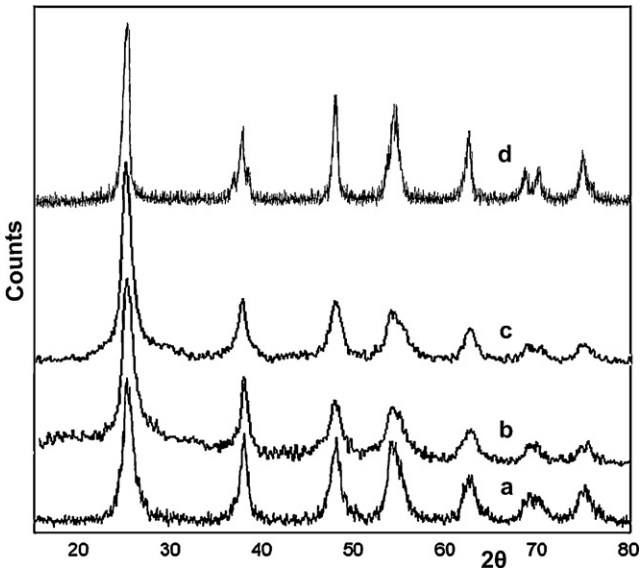

Fig. 4. XRD patterns of sol-derived powders at low temperature: (a) TiO_2, (b) Ag-doped TiO_2, (c) Zr-doped TiO_2 and (d) Ag–Zr-co-doped TiO_2.

samples. The absorption edge of the Ag–TiO_2 is about 475 nm, the band gap is estimated to be 2.61 eV, while the edge of the absorption of the Zr–TiO_2 samples is shifted to approximately 460 nm, corresponding to a band gap energy of 2.70 eV. The co-doped Ag–Zr–TiO_2 exhibit the largest visible light absorption among the four samples (Fig. 3a). The absorption edge of the Ag–Zr–TiO_2 sample has shifted to about 510 nm, corresponding to a band gap energy of 2.43 eV. While, the absorption onset for anatase TiO_2 coating is 400 nm, with band gap energy of 3.1 eV. The results indicate that visible light absorption of the TiO_2 is enhanced by introducing the Ag, Zr and the Ag–Zr co-doped. The best photocatalytic activity can be attained by the later one (the Ag–Zr co-doped) sample.

3.3. XRD analysis

The XRD patterns of pure, coated-fibers and sol-derived powders were recorded. The typical XRD reflections of the cellulosic fibers were identified [35]. Since the amount of TiO_2 was low on the fibers surface, the XRD patterns of TiO_2 and the doped TiO_2-coated fibers show a low intensity for the characteristics reflections of anatase phase.

Fig. 4 shows XRD patterns of sol–gel derived TiO_2, Ag-doped TiO_2, Zr-doped TiO_2, and Ag–Zr co-doped TiO_2 powders. As it is evident from the diffractograms, all the reflections belong to pure anatase phase and no additional reflections belonging to other phases are observed. These observations indicate that there is virtually no phase change in TiO_2 structure in the process of doping or co-doping. The relatively high width of the reflections associated with the TiO_2 phase suggests that the size of the particles is quite small. It is observed that doping of Ag and Zr reduced the grain size and enlarged the surface areas of nanoparticles. The average grain size are calculated using the Scherrer's equation based on the full width at half-maximum (FWHM) of the (1 0 1) peak of the compounds. The crystallite size, on the other hand, has been reduced with the doping as indicated by the peak broadening in the XRD patterns of Ag–TiO_2 and Zr–TiO_2 (Table 1). From Fig. 4b and c, it can be seen that the width of anatase 1 0 1 crystal plane reflection broadened as the silver and zirconium doping were added.

The phase structure, crystallite size and crystallinity of TiO_2 play an important role in photocatalytic activity. Many studies have confirmed that the anatase phase of titania shows higher photocatalytic activity than the brookite or rutile phases [36]. From the wide angle XRD patterns (Fig. 4), the titania and titania nanocomposites exist only in anatase phase. The anatase phase of the samples did not change prior and after using dopants, illustrating that doping and co-doping process did not change the catalysts structure or its crystallinity. The smaller crystallite size indicates that the preparation method used in the present work can effectively prompt the crystallization and inhibit the grain growth.

Our nano TiO_2 and the doped nano TiO_2 were prepared in the presence of acetic acid. This is due to the fact that protonation of TiO_2 nano particles can prevent further crystallization. In addition, the excess acetate anion adsorbed on the surface of TiO_2 could also suppress the growth of nano TiO_2. This role of acetate anion on the surface of TiO_2 could be responsible for the decrease in the crystallite size of TiO_2 during the sol–gel synthesis [4].

Fig. 4 displays that, characteristic peaks broadened when the ions doped into TiO_2. The ionic radius of the dopant ion is the most important factor, which strongly influence the ability of the dopant to enter into TiO_2 crystal lattice. If the ionic radius of the doping metal ions matches those of the lattice metal ion in oxides, the doping metal ion will substitute itself for the lattice in the doping reactive process (substitutional mode). While if the ionic radius of the dopant is much bigger or smaller than that of Ti^{4+}, the dopant substituting for TiO_2 crystal lattice ions must result into crystal lattice distortion [19].

The ionic radius of Ag^+ (0.115 nm) is bigger than that of Ti^{4+} (0.061 nm). Therefore, it is difficult for Ag^+ to really enter into the lattice of TiO_2. However, the electronegativity and the ionic radius of Zr^{4+} ion (1.4, 0.072 nm, respectively) are closer to those of Ti^{4+} ion (1.5, 0.061 nm). Therefore, it would be possible that Zr^{4+} ions replace lattice Ti^{4+} ions and thus occupy the lattice Ti^{4+} positions.

3.4. BET surface areas analysis

In general, the surface area of the catalyst is the most important factor influencing the catalytic activity. The surface area of nanoparticles was determined using the nitrogen gas adsorption method. Table 1 summarizes the BET surface areas and pore volumes of TiO_2, Ag–TiO_2, Zr–TiO_2, and Ag–Zr–TiO_2. It is obvious from the table that all the prepared samples have very high surface area compared to that of Degussa–TiO_2. TiO_2 nanoparticles have an average particle size of 5 nm and BET surface area of about 350 $m^2\ g^{-1}$, while Ag–TiO_2 nanoparticles show a diameter of <5 nm, and BET surface area about 372 $m^2\ g^{-1}$. Therefore, photoactivity of Ag–TiO_2 nanoparticles onto surface of fibers is higher than that of TiO_2 nanoparticles. The doping by Ag^+ ion slightly increases surface area and pore volume of TiO_2, whereas, doping by Zr^{4+} and co-doping process decrease slightly the surface area of Zr–TiO_2, and Ag–Zr–TiO_2. This observation confirms the possible mesoporous nature of the synthesized TiO_2 and TiO_2 nanocomposites.

3.5. Photocatalytic self-cleaning activity

The photocatalytic activities (self-cleaning test) of the prepared TiO_2 nanocomposite/fibers were studied by the degradation experiments using MB and Eosin Y dyes as model compound, because these have strong adsorption characteristics on many surfaces, good resistance to light degradation and a well defined optical absorption maxima in the visible region. There are several methods for evaluating the photocatalytic activity of self-cleaning materials. Three of the mostly used methods are the dye method [37,38], the stearic acid method [39], and the contact angle method [40]. Recently, Guan et al. [41] have reported a method using the 7-hydroxycoumarin probe, to evaluate the photocatalytic activity of self-cleaning materials. This method is based on monitoring of a highly fluorescent product generated by the self-cleaning materials following UV illumination. In the dye method, the whole process

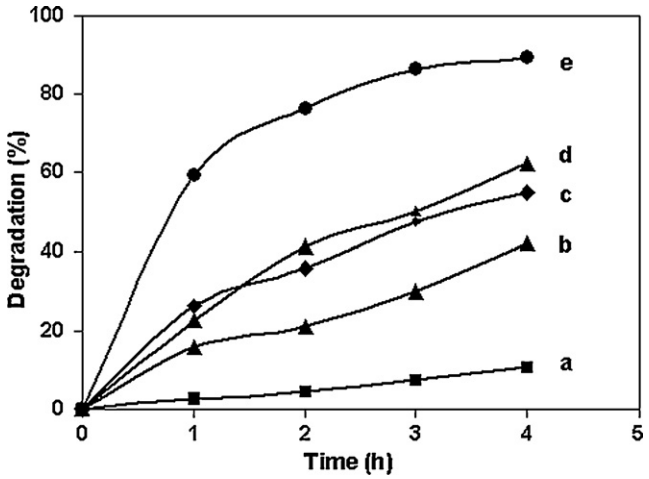

Fig. 5. Photocatalytic decomposition rate of MB against irradiation time. (a) MB on untreated fiber (b) MB on TiO_2 coated fiber (c) MB on Ag–TiO_2 coated fiber (d) MB on Zr–TiO_2 coated fiber and (e) MB on Ag–Zr–TiO_2 coated fiber.

of the photodegradation of dyes under UV irradiation is monitored, and the performance of self-cleaning materials is evaluated with the aid of the decolouration of dyes.

The photocatalytic activity of our synthesized TiO_2 nanocomposites on fibers was investigated by exposing the samples containing pre-adsorbed methylene blue (MB, cationic dye) and Eosin Y (anionic dye) to UV–Vis light. All the TiO_2-coated samples possessed the ability to decompose dyes upon UV–Vis irradiation. The UV–Vis reflectance spectra obtained on the coated samples with dyes prior and after illumination were recorded. The absorption peaks, corresponding to the dyes, diminished under reaction which indicates that the dyes were degraded. No new absorption bands appear in the visible regions. The disappearance rate of the bands due to MB and Eosin Y adsorbed on the TiO_2-covered fibers is much higher than those observed for the untreated fibers (Figs. 5a, b and 6a, b). This is not unexpected since the photocatalytic activity of TiO_2 is well known. Also, irradiation of all the doped TiO_2-fibers samples show enhanced photocatalytic activities, comparing with the TiO_2 coated fibers (Figs. 5c, d and 6c, d). The Zr–TiO_2 and Ag–TiO_2 samples exhibit a much higher efficiency in the degradation of dyes than pure TiO_2. In particular, Ag–Zr–TiO_2 shows the highest photocatalytic activity among all the samples (Figs. 5e and 6e). It has been demonstrated that incorporating Zr^{4+} into TiO_2 can introduce lattice defects and lead to higher photoactivities than those of the pure oxide [5]. The higher photoactivity of Ag–TiO_2 coating will be related to the existence of silver atom which are responsible for transporting more holes to the surface and enhance the photocatalytic efficiency [42].

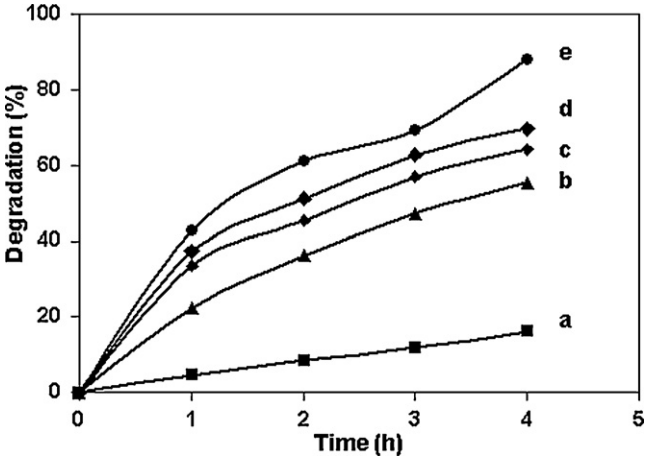

Fig. 6. Photocatalytic decomposition rate of EY against irradiation time. (a) EY on untreated fiber (b) EY on TiO_2 coated fiber (c) EY on Ag–TiO_2 coated fiber (d) EY on Zr–TiO_2 coated fiber and (e) EY on Ag–Zr–TiO_2 coated fiber.

The co-doped (Ag–Zr) TiO_2 exhibits highest photocatalytic activity, which is believed to be due to the synergistic effect between the Ag and the Zr doped into TiO_2 lattice. A strong Ag–Zr synergistic interaction appears to play a decisive role in driving the excellent photoactivity performance of Ag–Zr co-doped materials by affecting (i) electronic properties, particularly maximum decrease of the anatase band gap and subsequently enhancing the visible light photon absorption, and (ii) surface properties, in turn related to the formation of active radicals upon light irradiation.

4. Conclusions

Cellulosic fibers coated with nanocomposites of Ag–TiO_2, Zr–TiO_2, and Ag–Zr–TiO_2 show improved photodecomposition of dyes for self-cleaning applications. Photocatalytic self-cleaning potential of the nanocomposites prepared was assessed by photodegradation of MB and EY under UV–Vis light. The materials showed photocatalytic activity originated from TiO_2, doped and co-doped TiO_2 on their surface. In the all samples anatase TiO_2 nanoparticles with small particles size and high surface area are assisting for the observed enhanced photoactivity. In the photodecomposition of MB and EY, Ag–Zr–TiO_2 coated fiber showed the highest photocatalytic efficiency as compared to that of other nanocomposites. The excessive activity of the co-doped Ag–Zr TiO_2-coted fibers is believed to be due to the synergistic effect between the Ag and the Zr doped into TiO_2 lattice. Such strong effect supposed to be related to effective inhabitation of the recombination of photogenerated electrons and holes and creation of an increased concentration of active radical species.

Acknowledgements

The authors are grateful to University of Guilan for financial assistance of this research project.

References

[1] N. Sobana, M. Muruganadham, M. Swaminathan, Nano-Ag particles doped TiO_2 for efficient photodegradation of direct azo dyes, J. Mol. Catal. A: Chem. 258 (2006) 124–132.
[2] H.E. Chao, Y.U. Yun, H.U. Xiangfang, A. Larbot, Effect of silver doping on the phase transformation and grain growth of sol–gel titania powder, J. Eur. Ceram. Soc. 23 (2003) 1457–1464.
[3] D. Chatterjee, S. Dasguptha, Visible light induced photocatalytic degradation of organic pollutants, J. Photochem. Photobiol. C: Photochem. Rev. 6 (2005) 186–205.
[4] N. Venkatachalam, M. Palanichamy, V. Murugesan, Sol–gel preparation and characterization of alkaline earth metal doped nano TiO_2: efficient photocatalytic degradation of 4-chlorophenol, J. Mol. Catal. A: Chem. 273 (2007) 177–185.
[5] S. Chang, R. Doong, Characterization of Zr-doped TiO_2 nanocrystals prepared by a nonhydrolytic sol–gel method at high temperatures, J. Phys. Chem. B 110 (2006) 20808–20814.
[6] B. Gao, T.M. Lim, D.P. Subagio, T. Lim, Zr-doped TiO_2 for enhanced photocatalytic degradation of bisphenol A, Appl. Catal. A 375 (2010) 107–115.
[7] H.S. Hilal, L.Z. Majjad, N. Zaatar, A. El-Hamouz, Dye-effect in TiO_2 catalyzed contaminant photo-degradation: sensitization vs. charge-transfer formalism, Solid State Sci. 9 (2007) 9–15.
[8] A. Fujishima, T.N. Rao, D.A. Tryk, Titanium dioxide photocatalysis, J. Photochem. Photobiol. C: Photochem. Rev. 1 (2000) 1–35.
[9] A.H. Zyouda, N. Zaatara, I. Saadeddina, C. Ali, D. Parkc, G. Campetc, H.S. Hilal, CdS-sensitized TiO_2 in phenazopyridine photo-degradation: catalyst efficiency, stability and feasibility assessment, J. Hazard. Mater. 173 (2010) 318–325.
[10] W. Zhao, Z. Bai, A. Ren, B. Guo, C. Wu, Sunlight photocatalytic activity of CdS modified TiO_2 loaded on activated carbon fibers, Appl. Surf. Sci. 256 (2010) 3493–3498.

[11] J. Bai, J. Li, Y. Liu, B. Zhou, W. Cai, A new glass substrate photoelectrocatalytic electrode for efficient visible-light hydrogen production: CdS sensitized TiO_2 nanotube arrays, Appl. Catal. B: Environ. 95 (2010) 408–413.
[12] V. Subramanian, E. Wolf, P. Kamat, Semiconductor–metal composite nanostructures. To what extent do metal nanoparticles improve the photocatalytic activity of TiO_2 films? J. Phys. Chem. B 105 (2001) 11439–11446.
[13] A. Dobosz, A. Sobczynski, The influence of silver additives on titania photoactivity in the photooxidation of phenol, Water Res. 37 (2003) 1489–1496.
[14] D. Hufschmidt, D. Bahnemann, J.J. Testa, C.A. Emilio, M.I. Litter, Enhancement of the photocatalytic activity of various TiO_2 materials by platinisation, J. Photochem. Photobiol. A: Chem. 148 (2002) 223–231.
[15] J. Arana, J.M. Dona-Rodriguez, O. Gonzalez Diaz, E. Tello Rendon, J.A. Herrera Melian, G. Colon, J.A. Navio, J. Perez Pena, Gas-phase ethanol photocatalytic degradation study with TiO_2 doped with Fe, Pd and Cu, J. Mol. Catal. A: Chem. 215 (2004) 153.
[16] X.-Z. Shen, Z.-C. Liu, S.-M. Xie, J. Guo, Degradation of nitrobenzene using titania photocatalyst co-doped with nitrogen and cerium under visible light illumination, J. Hazard. Mater. 162 (2009) 1193–1198.
[17] Z.H. Yuan, J.H. Jia, L.D. Zhang, Influence of co-doping of Zn(II) + Fe(III) on the photocatalytic activity of TiO_2 for phenol degradation, Mater. Chem. Phys. 73 (2002) 323–326.
[18] L. Lin, R.Y. Zheng, J.L. Xie, Y.X. Zhu, Y.C. Xie, Synthesis and characterization of phosphor and nitrogen co-doped titania, Appl. Catal. B 76 (2007) 196–202.
[19] A.F. Shojaie, M.H. Loghmani, La^{3+} and Zr^{4+} co-doped anatase nano TiO_2 by sol-microwave method, Chem. Eng. J. 157 (2010) 263–269.
[20] Q. Xua, D.V. Welliaa, M.A. Ska, K.H. Lima, J.S.C. Loob, D.W. Liaoc, R. Amald, T.T.Y. Tan, Transparent visible light activated C–N–F-codoped TiO_2 films for self-cleaning applications, J. Photochem. Photobiol. A: Chem. 210 (2010) 181–187.
[21] J.H. Xu, J. Li, W.L. Dai, Y. Cao, H. Li, K. Fan, Simple fabrication of twist-like helix N,S-codoped titania photocatalyst with visible-light response, Appl. Catal. B: Environ. 79 (2008) 72–80.
[22] G. Liu, Y. Zhao, C. Sun, F. Li, G.Q. Lu, H.M. Cheng, Synergistic effects of B/N doping on the visible-light photocatalytic activity of mesoporous TiO_2, Angew. Chem. Int. Ed. 47 (2008) 4516–14516.
[23] X. Yang, C. Cao, L. Erickson, K. Hohn, R. Maghirang, K. Klabunde, Synthesis of visible-light-active TiO_2-based photocatalysts by carbon and nitrogen doping, J. Catal. 260 (2008) 128–133.
[24] C. Di Valentin, E. Finazzi, G. Pacchioni, Density functional theory and electron paramagnetic resonance study on the effect of N–F co-doping of TiO_2, Chem. Mater. 20 (2008) 3706–3714.
[25] D. Mihailovic, Z. Šaponjić, M. Radoičić, T. Radetić, P. Jovančić, J. Nedeljković, M. Radetic, Functionalization of polyester fabrics with alginates and TiO_2 nanoparticles, Carbohydr. Polym. 79 (2010) 526–532.
[26] H.F. Moafi, A.F. Shojaie, M.A. Zanjanchi, The comparison of photocatalytic activity of synthesized TiO_2 and ZrO_2 nanosize onto wool fibers, Appl. Surf. Sci. 256 (2010) 4310–4316.
[27] E. Allain, S. Besson, C. Durand, M. Moreau, T. Gacoin, J.P. Boilot, Transparent mesoporous nanocomposite films for self-cleaning applications, Adv. Funct. Mater. 17 (2007) 549–554.
[28] W.S. Tung, W.A. Daoud, Photocatalytic self-cleaning keratins: a feasibility study, Acta. Biomater. 5 (2009) 50–56.
[29] D. Wu, M. Long, J. Zhou, W. Cai, X. Zhu, C. Chen, Y. Wu, Synthesis and characterization of self-cleaning cotton fabrics modified by TiO_2 through a facile approach, Surf. Coat. Technol. 203 (2009) 3728–3733.
[30] M.I. Mejía, J.M. Marín, G. Restrepo, C. Pulgarín, E. Mielczarski, J. Mielczarski, Y. Arroyo, J.-C. Lavanchy, J. Kiwi, Self-cleaning modified TiO_2–cotton pretreated by UVC-light (185 nm) and RF-plasma in vacuum and also under atmospheric pressure, Appl. Catal. B: Environ. 91 (2009) 481–488.
[31] J. Yang, Y. Han, J. Choy, TiO_2 thin-films on polymer substrates and their photocatalytic activity, Thin Solid Films 495 (2006) 266–271.
[32] M.J. Uddin, F. Cesano, F. Bonino, S. Bordiga, G. Spoto, D. Scarano, et al., Photoactive TiO_2 films on cellulose fibres: synthesis and characterization, J. Photochem. Photobiol. A: Chem. 189 (2007) 286–294.
[33] J. Shi, S. Shang, L. Yang, J. Yan, Morphology and crystalline phase-controllable synthesis of TiO_2 and their morphology-dependent photocatalytic properties, J. Alloys Compd. 479 (2009) 436–439.
[34] N. Sobana, M. Muruganadham1, M. Swaminathan, Nano-Ag particles doped TiO_2 for efficient photodegradation of direct azo dyes, J. Mol. Catal. A: Chem. 258 (2006) 124–132.
[35] M.A. Moharram, T.Z.A.E. Nasr, N.A. Hakeem, X-Ray diffraction and infrared studies on the effect of thermal treatments on cotton celluloses I and II, J. Polym. Sci. Polym. Lett. Ed. 19 (1981) 183–187.
[36] M. Grandcolas, M.K.L. Du, F.B.A. Louvet, N. Keller, V. Keller, Porogen template assisted TiO_2 rutile coupled nanomaterials for improved visible and solar light photocatalytic applications, Catal. Lett. 123 (2008) 65–77.
[37] X. Wu, W. Qin, X. Ding, Y. Wen, H. Liu, Z. Jiang, Photocatalytic activity of Eu-doped TiO_2 ceramic films prepared by microplasma oxidation method, J. Phys. Chem. Solids 68 (2007) 2387–2393.
[38] S. Yew, H. Tang, K. Sudesh, Photocatalytic activity and biodegradation of polyhydroxybutyrate films containing titanium dioxide, Polym. Degrad. Stab. 91 (2006) 1800–1807.
[39] A. Mills, J. Wang, Simultaneous monitoring of the destruction of stearic acid and generation of carbon dioxide by self-cleaning semiconductor photocatalytic films, J. Photochem. Photobiol. A: Chem. 182 (2006) 181–186.
[40] J. Zhao, L. Xu, J. Yu, Z. Lv, Q. Yuan, Chinese Patent CN, 1,603,786A (2005).
[41] H. Guan, L. Zhu, H. Zhou, H. Tang, Rapid probing of photocatalytic activity on titania-based self-cleaning materials using 7-hydroxycoumarin fluorescent probe, Anal. Chim. Acta 608 (2008) 73–78.
[42] X. Houa, M. Huanga, X. Wub, A. Liub, Preparation and studies of photocatalytic silver-loaded TiO_2 films by hybrid sol–gel method, Chem. Eng. J. 146 (2009) 42–48.